Kelvin Wong,
Chipan Tam, and Michael Ng

Accurate Vascular Delay Estimation from Low-Temporal Resolution Image Data Set

Magnetic resonance perfusion (MRP) imaging is a widely used clinical imaging technique to determine how blood flows through biological tissue. Due to the generic nature of MRP, its application extends from the brain and heart to any other organ in the body. The most important application of MRP is to determine if the tissue of interest lacks blood flow. A major focus is on the ischemic stroke, which is a lack of blood in the brain tissue due to blood vessel blockage, and the myocardial ischemia, which is the lack of blood in the heart muscle tissue. This article will discuss MRP for the brain tissue. A detailed description of the challenges is provided next.

MRP IMAGING OF BRAIN TISSUE

MRP of the brain is conducted by taking a three-dimensional (3-D) image volume of the brain at low-temporal resolution every 1–2 s repeatedly, over a period of 1–2 min using a magnetic resonance imaging system. During imaging, a chemical dye is injected very quickly into the patient's vein. Dynamic 3-D imaging is used to monitor the traversal of the dye through the brain tissue. This idea is similar to using a Dirac delta function to probe the system response; in this case, the transfer function of living human brain tissue. Until recently [1], it has been traditionally difficult to recover the transfer function accurately because of the low-temporal resolution of imaging. In addition, there has been a biased misconception in the field that a delay in the arrival of blood supply to the brain tissue is not as important compared to the amount of blood flowing through it. However, recent studies have shown that the time it takes for blood to traverse from the artery to the tissue of interest, or arterial-tissue delay (Tmax), is strongly predictive of tissue fates of whether ischemic tissue will be salvageable or not [2]. Unfortunately, few methods are available [3], [4] that can provide an accurate estimate of Tmax in clinical settings, primarily due to the low-temporal resolution of imaging. In this article, we will first review the recent work done in the field, followed by dissecting the Tmax estimation problem, and discuss how we can get an accurate and stable estimate without the need of a high-temporal resolution data set. We will prove the accuracy and robustness of the method over a large range of physiological parameters using Monte Carlo simulation. Furthermore, we will illustrate the result using data from real human brain tumor cases.

CONVERTING IMAGE INTENSITY TO CONTRAST CONCENTRATION

In MRP studies, we can convert the image pixel intensity to amount of dye in the tissue. The relationship between signal intensity-time curve, $S(t)$, and concentration-time curve, $C(t)$, during passage of a dye is

$$S(t) = S_0 \exp(-k \cdot C(t) \cdot TE), \quad (1)$$

where S_0 is the image intensity before dye injection. The relationship between $C(t)$ and the arterial input function, $AIF(t)$, which describes the concentration-time curve of the dye in the arterial blood, can be modeled by the following convolution [5]:

$$\begin{aligned} C(t) &= \mathrm{CBF} \cdot AIF(t) \otimes R(t) \\ &= \mathrm{CBF} \cdot \int_{t_0}^{t} AIF(\tau) \cdot R(t-\tau) d\tau, \end{aligned} \quad (2)$$

where $R(t)$ is the tissue residue function.

The integral (2) can be solved by integral transform directly or simply numerically approximated by rectangular rule [5] by incorporating the delay in the formulation using a global $AIF(t)$, as shown by (3), found at the bottom of the page, where Δt is the sampling interval, t_0 is the bolus arrival time, d is the delay and $R(d) = 1$. Equation (3) can be simplified to $\mathbf{c} = \mathbf{A} \cdot \mathbf{r}$ by multiplying $R(t)$ by the cerebral blood flow (CBF). The deconvolution problem is then reduced to finding the matrix inverse of A. CBF is calculated as the maximum value of r and by central volume theorem

$$\begin{bmatrix} C(t_0+d) \\ C(t_1+d) \\ \vdots \\ C(t_{N-1}+d) \end{bmatrix} = \Delta t \begin{bmatrix} AIF(t_0) & 0 & \cdots & 0 \\ AIF(t_1) & AIF(t_0) & \cdots & 0 \\ \vdots & \vdots & \ddots & \vdots \\ AIF(t_{N-1}) & AIF(t_{N-2}) & \cdots & AIF(t_0) \end{bmatrix} \times \begin{bmatrix} R(d) \\ R(t_1-t_0+d) \\ \vdots \\ R(t_{N-1}-t_0+d) \end{bmatrix} \cdot \mathrm{CBF}. \quad (3)$$

Digital Object Identifier 10.1109/MSP.2010.936059

[5], mean transit time (MTT) is calculated by

$$\mathrm{MTT} = \int_0^\infty t \cdot h(\tau) d\tau.$$

ESTIMATING THE TIME DELAY FROM ARTERY TO TISSUE

The time delay for blood to flow from the artery to the tissue, Tmax, can be ideally determined by the time delay the dye first appears in the artery and tissue. However, in the presence of noise, this delay estimation is sensitive to signal-to-noise ratio (SNR) [3]. Cheong et al. [4] proposed bolus arrival time estimation methods by using piece-wise continuous regression models, which can be used for delay estimation. Rose et al. [6] proposed a geometric-based method for delay estimation and demonstrated that it improved the results for acute stroke treatment after delay correction. Ibaraki et al. [3] introduced zero-delay singular value decomposition (ZD-SVD) with a new delay estimation method. Pixel-by-pixel least squares estimation was used to fit the delay between $AIF(t)$ and $C(t)$. However, these delay estimation algorithms are based on $C(t)$, which are highly sensitive to the temporal SNR of the source images compared to the delay insensitive method such as reformatted singular value decomposition (rSVD) [7]. In this article, we discuss a regularization-based delay estimation (RDE) method that allows accurate and stable Tmax estimation compared to the ZD-SVD method.

THE RDE METHOD

The RDE method is a two-step method to estimate delay accurately using the deconvolution approach. First, the concentration time curve is shifted along the time axis. Delay can be roughly estimated by the maximal shift value such that the peak of the corresponding deconvoluted solution $R(t)$ is located at $R(0)$, i.e.,

$$\bar{d} = -\arg\max_{s\in[-4,6]} \{R_s(0) = \max(R_s)\}, \quad (4)$$

where R_s is the estimated tissue residue function corresponds to $C(t)$ with shift s.

To estimate delay accurately, concentration time curves $C(t)$ were generated using $TR = 1$ s and 2 s and the curves were interpolated to 0.1 s temporal resolution by cubic spline. Tikhonov regularization [8] is used to generate a number of solutions of $R_s(t)$ corresponding to pixel-by-pixel shifted $C(t)$ from –8 to + 6 s every 0.1 s to cover a large physiological range of delay. The Volterra convolution method [9] is then used to reduce the discretization error in delay estimation using $R(t)$ after interpolation. It has been demonstrated that Volterra convolution is the most accurate discretization method for delay correction approach compared with other methods when there is only small amount of delay in $C(t)$ [9].

Owing to the fact that the shape of $R(t)$ may be distorted due to regularization error, Tmax has a strong dependence on MTT. We estimated the bias of delay during delay estimation for different λ and MTT of $R(t)$ with an exponential form by Monte Carlo simulation. The estimated delay correction factor f was defined as

$$f(\lambda, \overline{\mathrm{MTT}}) = m(\lambda) \cdot \overline{\mathrm{MTT}} + c(\lambda), \quad (5)$$

where m and c are estimated by fitting delay estimation errors from a range of MTT and a fixed λ. $\overline{\mathrm{MTT}}$ is determined by $\overline{R(t)}$, which is estimated by rSVD [7] where $\overline{\mathrm{MTT}} = \sum \overline{R}(t)/\max(\overline{R}(t))$. In our delay estimation algorithm, $\overline{R(t)}$ was first estimated by rSVD [7]. Then, the correction factor f obtained from (5) is added to the result obtained from (6) as the finalized estimated delay.

We compared the performance of delay estimation accuracy of our method with an advanced delay estimation algorithm, ZD-SVD [3]. ZD-SVD estimates delay d by fitting $C(t)$ with a convolution of $AIF(t)$ and an exponential function

$$\bar{d} = \arg\min_d \|C(t) - aAIF(t-d) \otimes \exp(-bt)\|_2^2. \quad (6)$$

SIMULATED PERFORMANCE OF THE RDE METHOD

Monte Carlo simulation was used to simulate a large physiological range according to a previous publication [1] to evaluate the accuracy of the delay estimation method. Delay was simulated with the range of -4 to $+6$ s every 0.5 s. MTT was simulated ranging from 3.4–24 s. Temporal resolution ranged from 1–2 s and was set to 1 s in the experiments unless otherwise specified. Optimal thresholds of the singular value were set to 10% of the max singular value for ZD-SVD [10] and λ were set to 0.7 and 1.5 corresponding to SNR = 100 and 50, respectively. Simulations were repeated 100 times and mean and standard deviation (SD) of the results were computed.

Simulation results show that there is a linear relationship between the correction factor f obtained (5) and estimated MTT and the slope of the line varies with different λ. At 1 s or 2 s temporal resolution, the estimated delay with the proposed RDE method is more accurate and stable than the ZD-SVD method. The result is summarized in Table 1.

CLINICAL VALIDATION OF THE RDE METHOD

Two MRP cases were used as validation in this study. Both have significant regional vascular delay. The first case was from a brain tumor patient where multislice perfusion images were acquired every 2 s. The second case was from a cerebral vasculitis patient with perfusion images acquired every 1.9 s. The baseline SNR of the first and second case is 100 and 50, respectively. The extensive regional vascular delay is a good validation method as local regional delay is rather constant.

The Tmax map was computed for both patients for all multislice images, and the representative results are shown in Figure 1. In the brain tumor patient case [Figure 1(a)], which has a baseline image SNR of 100, the Tmax delays estimated by the RDE and ZD-SVD

methods were almost identical although the Tmax map of the ZD-SVD method is slightly noisier indicated by more spatial variation in the Tmax map. Both methods indicated the large delay region in Figure 1(a) of the Tmax delay map clearly (left-right flipped in radiological convention). In the vasculitis case [Figure 1(b)], which has a regional delay with baseline image SNR of 50, both algorithms indicated similar results for delay estimation but the Tmax map from the ZD-SVD method were much noisier than the RDE method.

[TABLE 1] MEAN ±SD OF ESTIMATED DELAY OF ZD-SVD AND RDE METHODS. SIMULATIONS ARE BASED ON THE SPECIFIC CONDITIONS OF MTT RANGING FROM 3.4 S TO 24 S AND DIFFERENT *R* MODELS.

SIMULATION CONDITIONS	ZD-SVD	RDE
Exponential $R(t)$ Model: TR = 1 s, SNR = 100, CBV = 4%, MTT = 3.4 s to 24 s	0.37 ± 0.15 to 0.25 ± 0.35	−0.02 ± 0.08 to 0.01 ± 0.30
Linear $R(t)$ Model: TR = 1 s, SNR = 100, CBV = 4%, MTT = 3.4 s to 24 s	0.46 ± 0.13 to 0.28 ± 0.30	0.11 ± 0.07 to 0.01 ± 0.31
Exponential $R(t)$ Model: TR = 1 s, SNR = 50, CBV = 4%, MTT = 3.4 s to 24 s	0.18 ± 0.32 to −0.02 ± 0.92	−0.03 ± 0.13 to −0.11 ± 0.41
Linear $R(t)$ Model: TR = 1 s, SNR = 50, CBV = 4%, MTT = 3.4 s to 24 s	0.34 ± 0.32 to 0.02 ± 0.85	0.21 ± 0.13 to −0.16 ± 0.57
Exponential $R(t)$ Model: TR = 2 s, SNR = 100, CBV = 4%, MTT = 3.4 s to 24 s	0.90 ± 0.19 to 0.82 ± 0.44	−0.10 ± 0.10 to −0.07 ± 0.38
Linear $R(t)$ Model: TR = 2 s, SNR = 100, CBV = 4%, MTT = 3.4 s to 24 s	1.02 ± 0.15 to 0.77 ± 0.40	0.08 ± 0.07 to −0.15 ± 0.35
Exponential $R(t)$ Model: TR = 2 s, SNR = 50, CBV = 4%, MTT = 3.4 s to 24 s	0.78 ± 0.44 to 0.45 ± 0.98	−0.10 ± 0.19 to −0.10 ± 0.61
Linear $R(t)$ Model: TR = 2 s, SNR = 50, CBV = 4%, MTT = 3.4 s to 24 s	0.93 ± 0.34 to 0.35 ± 1.43	0.07 ± 0.15 to 0.01 ± 0.71

LIMITATIONS OF THE RDE METHOD

Delay estimation is a challenging problem in MRP. It depends on the distribution of $AIF(t)$ and $R(t)$ because $C(t)$ is a result of $AIF(t) \otimes R(t)$. Since $R(t)$ is an unknown in practice, it is difficult to obtain exact the delay from the concentration time curve. Also, the most common TR in MRP is 1–2 s, which limits the accuracy of the delay estimation algorithms. Both the ZD-SVD and RDE methods require interpolation to increase the accuracy of delay estimation that may introduce bias into signals. However, this problem may be reduced since the magnetic resonance imaging technique is improving. Delay estimation could also be provided by using the location of the peak in estimated $R(t)$. However, as the errors introduced in discretization and regularization, the estimated delay is always seriously biased and the situation is more serious for prolonged MTT [10].

Discretization error is an error introduced for approximating (2). Volterra can reduce it significantly compared with a rectangular rule based on the assumption that $R(t)$ is differentiable for the case without delay. On the other hand, it can be further reduced by decreasing temporal resolution, which can benefit from developing parallel or sparse imaging technology. Interpolation is also a promising approach although it may distort the original signal. Monte Carlo simulations and clinical applications should be considered to further validate the effects of interpolation for CBF and delay estimation.

Finally, the application of the RDE method is limited by a few assumptions on the contrast concentration-time curve, $C(t)$, that it contains only the first pass of the dye. We may not handle some common issues in $C(t)$, e.g., recirculation and leakage, unless appropriate corrections are addressed. Also, imperfect data may have some unexpected distortions in $C(t)$, e.g., negative $C(t)$ before or after first pass, may significantly reduce the accuracy of delay correction methods since delay estimation are highly dependent on the information from the first pass.

SUMMARY

In this article, we discussed a strategy to recover the high-temporal resolution signal from the low-temporal resolution source data in a discretized ill-posed matrix inverse problem. In this particular application, we determine the delay of blood supply to different brain regions using the perfusion imaging method, which is of critical importance to predict tissue health status in acute stroke patients and to select the best therapy. Current acute stroke clinical trials in general involved the use of Tmax and use it to select the group of patients for therapy. An accurate Tmax estimation reduces the uncertainty in patient selection and reduces the sample size to achieve significant clinical outcomes.

The problem described in this article is a common ill-posed matrix inverse problem in biomedical imaging and signal processing. For example, diffusion tensor computation in diffusion tensor imaging that allows one to noninvasively map out the wiring of human brain

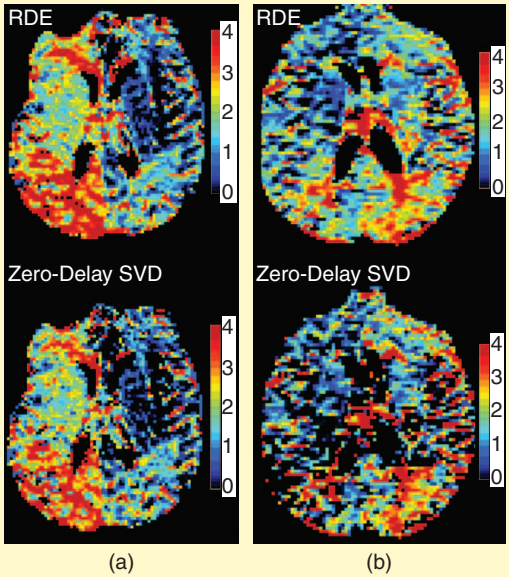

[FIG1] Tmax maps from RDE and ZD-SVD methods showed strong agreement when (a) baseline image SNR=100 while the RDE method showed better robustness to noise than the ZD-SVD method when (b) baseline image SNR=50.

is also an ill-posed matrix inverse problem. In that case, the solution should be constrained by physical properties of water diffusion in white matter fibers in the brain. Solving these problems usually require a multidisciplinary approach by taking advantages of domain knowledge, be it in biomedical imaging, physics, or physiology with advanced signal processing strategies.

AUTHORS

Kelvin Wong (kwong@tmhs.org) is an assistant professor of electronic engineering in radiology at Weill Cornell Medical College and adjunct assistant professor of pediatrics at Baylor College of Medicine. He is director of the Translational Multimodality Optical Imaging Lab, The Methodist Hospital Research Institute and codirector of the Small Animal Imaging Facility, Texas Children's Hospital.

Chipan Tam (cptam@math.hkbu.edu.hk) is a graduate researcher in the Department of Mathematics at Hong Kong Baptist University.

Michael Ng (mng@math.hkbu.edu.hk) is a professor in the Centre for Mathematical Imaging and Vision, as well as the Department of Mathematics at the Hong Kong Baptist University.

REFERENCES

[1] K. K. Wong, C. P. Tam, M. Ng, S. T. Wong, and G. S. Young, "Improved residue function and reduced flow dependence in MR perfusion using least-absolute-deviation regularization," *Magn. Reson. Med.*, vol. 61, pp. 418–428, Feb. 2009.

[2] J. M. Olivot, M. Mlynash, V. N. Thijs, S. Kemp, M. G. Lansberg, L. Wechsler, R. Bammer, M. P. Marks, and G. W. Albers, "Optimal Tmax threshold for predicting penumbral tissue in acute stroke," *Stroke*, vol. 40, pp. 469–475, Feb. 2009.

[3] M. Ibaraki, E. Shimosegawa, H. Toyoshima, K. Takahashi, S. Miura, and I. Kanno, "Tracer delay correction of cerebral blood flow with dynamic susceptibility contrast-enhanced MRI," *J. Cereb. Blood Flow Metab.*, vol. 25, pp. 378–390, Mar. 2005.

[4] L. H. Cheong, T. S. Koh, and Z. Hou, "An automatic approach for estimating bolus arrival time in dynamic contrast MRI using piecewise continuous regression models," *Phys. Med. Biol.*, vol. 48, pp. N83–N88, Mar. 2003.

[5] E. P. Xing, A. Y. Ng, M. I. Jordan, and S. Russell, "Distance metric learning with application to clustering with side-information," in *Advances in Neural Information Processing Systems 15*, S. Becker, S. Thrun, and K. Obermayer, Eds. Cambridge, MA: MIT Press, 2003, pp. 505–512.

[6] S. E. Rose, A. L. Janke, M. Griffin, S. Finnigan, and J. B. Chalk, "Improved prediction of final infarct volume using bolus delay-corrected perfusion-weighted MRI implications for the ischemic penumbra," *Stroke*, vol. 35, pp. 2466–2471, Nov. 2004.

[7] M. R. Smith, H. Lu, S. Trochet, and R. Frayne, "Removing the effect of SVD algorithmic artifacts present in quantitative MR perfusion studies," *Magn. Reson. Med.*, vol. 10, no. 2, pp. 631–634, Mar. 2004.

[8] F. Calamante, D. G. Gadian, and A. Connelly, "Quantification of bolus-tracking MRI: Improved characterization of the tissue residue function using Tikhonov regularization," *Magn. Reson. Med.*, vol. 50, pp. 1237–1247, Dec. 2003.

[9] S. Sourbron, R. Luypaert, D. Morhard, K. Seelos, M. Reiser, and M. Peller, "Deconvolution of bolus-tracking data: A comparison of discretization methods," *Phys. Med. Biol.*, vol. 52, pp. 6761–6778, Nov. 2007.

[10] L. Torresani and K.-C. Lee, "Large margin component analysis," in *Advances in Neural Information Processing Systems 19*, B. Schölkopf, J. Platt, and T. Hoffman, Eds. Cambridge, MA: MIT Press, 2007, pp. 1385–1392.

[11] G. Chechik, U. Shalit, V. Sharma, and S. Bengio, "An online algorithm for large scale image similarity learning," in *Advances in Neural Information Processing Systems 22*, Y. Bengio, D. Schuurmans, J. Lafferty, C. K. I. Williams, and A. Culotta, Eds. 2009, pp. 306–314.

SP

 continued from page 150

define a valid distance metric; second, because linear inequalities in the elements of this matrix can ensure that inputs are correctly labeled by kNN classification or Gaussian mixture modeling. Large-scale applications of these ideas are made possible by recent advances in numerical optimization [6]. Looking forward, we anticipate many such applications given the ubiquitous role of distance metrics in both nonparametric and parametric models of classification.

AUTHORS

Kilian Q. Weinberger (kilian@cse.wustl.edu) is an assistant professor in the Department of Computer Science and Engineering at Washington University, St. Louis.

Fei Sha (feisha@usc.edu) is an assistant professor in the Viterbi School of Engineering at the University of Southern California.

Lawrence K. Saul (saul@cs.ucsd.edu) is an associate professor in the Department of Computer Science and Engineering at the University of California San Diego.

REFERENCES

[1] R. Duda, P. Hart, and D. Stork, *Pattern Classification*. New York: Wiley, 2000.

[2] A. Globerson and S. Roweis, "Metric learning by collapsing classes," in *Advances in Neural Information Processing Systems 18*, Y. Weiss, B. Schölkopf, and J. Platt, Eds. Cambridge, MA: MIT Press, 2006, pp. 451–458.

[3] N. Shental, T. Hertz, D. Weinshall, and M. Pavel, "Adjustment learning and relevant component analysis," in *Proc. 7th European Conf. Computer Vision* (Lecture Notes in Computer Science), 2002, pp. 776–792.

[4] S. Shalev-Shwartz, Y. Singer, and A. Ng, "Online and batch learning of pseudo-metrics," in *Proc. 21st Int. Conf. Machine Learning (ICML'04)*, Banff, Canada, 2004, pp. 94–101.

[5] E. Xing, A. Ng, M. Jordan, and S. Russell, "Distance metric learning with application to clustering with side-information," in *Adv. Neural Inform. Process. Syst. 15*. Cambridge, MA: MIT Press, pp. 505–512, 2003.

[6] S. Boyd and L. Vandenberghe, *Convex Optimization*. Cambridge, U.K.: Cambridge Univ. Press, 2004.

[7] K. Weinberger and L. Saul, "Distance metric learning for large margin nearest neighbor classification," *J. Mach. Learn. Res.*, vol. 10, no. 2, pp. 207–244, 2009.

[8] F. Sha and L. K. Saul, "Large margin hidden Markov models for automatic speech recognition," in *Advances in Neural Information Processing Systems 19*, B. Schölkopf, J. Platt, and T. Hofmann, Eds. Cambridge, MA: MIT Press, 2007, pp. 1249–1256.

[9] B. Boser, I. Guyon, and V. Vapnik, "A training algorithm for optimal margin classifiers," in *Proc. 5th Annu. Workshop on Computational Learning Theory (COLT'02)*, Pittsburgh, PA, 1992, pp. 144–152.

[10] L. Torresani and K.-C. Lee, "Large margin component analysis," in *Adv. Neural Inform. Process. Syst. 19*, vol. 22, B. Schölkopf, J. Platt, and T. Hoffman, Eds. Cambridge, MA: MIT Press, pp. 1385–1392, 2007.

[11] G. Chechik, U. Shalit, V. Sharma, and S. Bengio, "An online algorithm for large scale image similarity learning," in *Advances in Neural Information Processing Systems 21*, Cambridge, MA: MIT Press, 2009, pp. 306–314.

[12] D. Tran, A. Sorokin, and D. Forsyth, "Human activity recognition with metric learning," in *Proc. European Conf. Computer Vision (ECCV'08)*, 2008, pp. 548–561.

SP